

2025-09-29

The self-archived post print version of this conference paper is available at Linköping University Institutional Repository (DiVA):

<https://urn.kb.se/resolve?urn=urn:nbn:se:liu:diva-218070>

Long-Term Evolution-based Time Synchronization in Distributed Sensor Networks

William Nordström, Magnus Malmström, Niclas Granström, Patrik Hedström, Ashwani Koul and Gustaf Hendeby

In: Proceedings of 28th International Conference on Information Fusion, 2025

ISBN: 978-1-0370-5623-9

Publisher: IEEE

<https://doi.org/10.23919/FUSION65864.2025.11124126>

N.B.: When citing this work, cite the original publication.

© 2025 IEEE. Personal use of this material is permitted. Permission from IEEE must be obtained for all other uses, in any current or future media, including reprinting/republishing this material for advertising or promotional purposes, creating new collective works, for resale or redistribution to servers or lists, or reuse of any copyrighted component of this work in other works.

Long-Term Evolution-based Time Synchronization in Distributed Sensor Networks

William Nordström[†], Magnus Malmström[†], Niclas Granström[†], Patrik Hedström[†], Ashwani Koul*, Gustaf Hendeby*

[†] Swedish Defence Research Agency (FOI)

Email: {firstname.lastname}@foi.se

* Linköping University (LiU)

Email: {firstname.lastname}@liu.se

Abstract—This paper investigates time synchronization in distributed sensor networks using the primary synchronization signal (PSS) in Long-Term Evolution (LTE). Two LTE-based time synchronization methods with receiver-to-receiver characteristics have been evaluated in simulations, the passive Scalable Wireless Network Synchronization (SWINS) and the active Reference Broadcast Synchronization (RBS). In addition, small scale hardware experiments were conducted for SWINS. Time synchronization is crucial for many applications, such as power grid monitoring, communication systems, and sensor data fusion. Global Navigation Satellite Systems (GNSS) are currently the state of the art for time synchronization in distributed wireless sensor networks. However, GNSS is vulnerable to jamming and spoofing, which requires alternative methods, e.g., using signals of opportunity. Both evaluated methods achieve accuracy comparable to GNSS in Matlab simulations with high SNR. SWINS performs better in synchronized LTE networks while RBS is superior in unsynchronized networks, which means that the LTE base station transmissions are not synchronous. The disturbance and sensitivity analysis indicates that joint clock offset and position estimation is preferable to sole clock offset estimation when the receiver position uncertainty exceeds 5 and 7 meters for SWINS and RBS respectively. The hardware experiments, using real experimental data, verify the simulation results by showing promising results and potential for real-world application.

Index Terms—Long-Term Evolution (LTE), Primary Synchronization Signal (PSS), time synchronization, distributed sensor networks, clock offset estimation, joint clock offset and position estimation, signal of opportunity

I. INTRODUCTION

Time synchronization in distributed sensor networks is vital for sensor fusion applications. Power grid monitoring is one example of an application where the significance of time synchronization has increased after the Northeast blackout of 2003 in the United States. An incident where asynchronous monitoring caused inadequate situational awareness preventing necessary measures [1] [2].

Currently, Global Navigation Satellite Systems (GNSS) are the state-of-the-art for obtaining time synchronization [3]. However, due to the vulnerability to jamming and spoofing, alternative time synchronization methods are of interest [4]. Self-transmission of a reference signal is a potential solution to the problem [5]. Although this could be effective, the reference transmitter is exposed and can be localized by adversaries,

which is a problem in a military context. Therefore, commonly available background signals, i.e., *signals of opportunity*, are of interest, e.g., radio and television broadcasting.

One possible source of signals of opportunity is LTE. Governmental and commercial solutions exist in 170 countries, allowing for LTE coverage in most populated areas around the globe. Standardization of the LTE protocol, according to 3GPP, is crucial to the world-wide use [6].

The LTE protocol is designed with a set of synchronization signals, used for synchronizing the radio frame at the receiver end. Naturally, research within the field of LTE started focusing on how to increase the likelihood of detecting the synchronization signals in suboptimal conditions. In [7], techniques for improving detection of the primary synchronization signal (PSS) in low SNR conditions and with large frequency offsets were investigated. The proposed algorithm showed good performance with low SNR and that frequency offset effects could be neglected. The radio frame synchronization was then improved upon by increasing the scope beyond the dedicated LTE synchronization signals, the PSS and the secondary synchronization signal (SSS). In [8], it is studied how radio frame timing can be enhanced by either fusing the PSS and SSS or using the specific cell reference identifier signals (CRS) for estimation. The CRS is typically used as pilots for channel estimation, but shows greater performance for radio frame synchronization due to transmission over the whole transmission bandwidth, which can be compared to the 62 center subcarriers of the PSS and SSS [8].

More recently, the LTE downlink has been utilized beyond radio frame synchronization as signals of opportunity in the fields of navigation and localization [9]–[12]. For example, [9] are using the CRS for vehicular positioning and [12] are using the combination of PSS, SSS, and CRS for improving TDOA-based navigation. Similarly, [10] compares the performance of SSS-based to CRS-based tracking for localization using a GNSS-based architecture, where correlation is calculated with a predefined sequence in the time domain. Hence, the LTE downlink shows promising potential to be utilized as a signal of opportunity in GNSS-denied environments. The scope of this paper is limited to only using the PSS as a signal of opportunity for synchronization.

This paper presents a novel application using the LTE

downlink as a source of signals of opportunity in a GNSS-denied scenario for multiple units, by extending the time synchronization application to distributed sensor networks. This is done by evaluating two methods and their sensitivity to different disturbances. The paper presents circumstance-based guidelines for using the selected methods. The emphasis of this paper is not to further improve on the state-of-the-art for LTE-based frame synchronization or single unit navigation, rather on expanding the application of the LTE downlink as a time synchronization reference for distributed sensor networks.

In this paper the PSS is used as signal of opportunity. Two methods are studied, namely Scalable Wireless Network Synchronization (SWINS) [13] and Reference Broadcast Synchronization (RBS) [14]. The selected methods were required to have receiver-to-receiver characteristics. Evaluation is done using Matlab simulations and small-scale hardware experiments using software-defined radio.

II. SYNCHRONIZATION METHODS

Some of the most popular time synchronization methods for wireless networks are RBS, Timing-sync Protocol for Sensor Networks (TPSN) [15], and Flooding Time Synchronization Protocol (FTSP) [15]. All three methods are active, which means that communication is required between the network nodes. Both TPSN and FTSP are sender-to-receiver synchronization methods, requiring more control of the LTE base stations (BS) [15]. This inhibits the use of these time synchronization methods, since LTE BS control is unrealistic. In contrast, RBS is a potential candidate since it is a receiver-to-receiver synchronization method, solely relying on receiver control. Beyond the active methods mentioned, the passive SWINS, relying on cyclic reference transmissions, is chosen for evaluation.

A. Scalable Wireless Network Synchronization

Scalable Wireless Networks Synchronization is a passive synchronization method not relying on communication within the sensor network, making the receivers less exposed and more difficult to localize [13]. Given an arbitrary cyclic synchronization or reference signal from a BS transmitter b , the method utilizes the i 'th cyclic signal arrival time t_i^b as a measurement according to

$$t_i^b(\tau, \mathbf{p}_{\text{Rx}}) = T_{\text{ref}} + (i-1)T_{\text{period}} + \tau + \frac{\|\mathbf{p}_{\text{Rx}} - \mathbf{p}_b\|}{c}, \quad (1)$$

where T_{ref} is a local reference time, T_{period} is the cyclic time of the reference signal, and τ is the receiver clock offset. The receiver position is \mathbf{p}_{Rx} and the BS transmitter position is \mathbf{p}_b . Given a sufficient set of BS transmitters \mathcal{B} and measurements y_i^b , $i = 1, 2, \dots, N$, of the synchronization signal arrival time for all transmitters in \mathcal{B} , the solution is given by minimizing

$$\sum_{b \in \mathcal{B}} \sum_{i=1}^N (y_i^b - t_i^b(\tau, \mathbf{p}_{\text{Rx}}))^2, \quad (2)$$

for each receiver, where the variables are the receiver clock offset error τ and position \mathbf{p}_{Rx} . Here, inter-BS synchronization is assumed.

B. Reference Broadcast Synchronization

Reference Broadcast Synchronization is an active synchronization method, where the received reference signal arrival times are communicated and compared within the sensor network [14]. Assuming inter-BS synchronization, the i 'th signal arrival time $t_{i,m}^b$ at a receiver m transmitted by BS b can be expressed as

$$t_{i,m}^b(\tau_m, \mathbf{p}_m) = T_{\text{Tx}} + \tau_m + \frac{\|\mathbf{p}_m - \mathbf{p}_b\|}{c}, \quad (3)$$

where T_{Tx} is the transmission time, and τ_m the receiver clock offset. The BS transmitter and receiver is positioned at \mathbf{p}_b and \mathbf{p}_k , respectively. Given that a reference signal has been received at two different receivers k and m , the pairwise arrival time difference between a sensor m and an arbitrary reference sensor k can be formed as

$$\Delta_{i,(m,k)}^b(\tau_m, \tau_k, \mathbf{p}_m, \mathbf{p}_k) \triangleq t_{i,m}^b(\tau_m, \mathbf{p}_m) - t_{i,k}^b(\tau_k, \mathbf{p}_k), \quad (4)$$

which is then used as a measurement in the synchronization method.

Given a set of BS transmitters \mathcal{B} , a set of sensors $m = 1, 2, \dots, M$, and a reference sensor k in the sensor set, the solution is given by minimizing

$$\sum_{\substack{m=1 \\ m \neq k}}^M \sum_{b \in \mathcal{B}} \sum_{i=1}^N (y_{i,(m,k)}^b - \Delta_{i,(m,k)}^b(\tau_m, \tau_k, \mathbf{p}_m, \mathbf{p}_k))^2, \quad (5)$$

where N is the number of synchronization signal detections. The optimization variables are the clock errors $\tau_m, \forall m$ and the sensor positions $\mathbf{p}_m, \forall m$.

C. Estimators

Two different estimators were applied for either sole clock offset estimation or joint clock offset and sensor position estimation. When the positions of both the BSs and the sensors are known, the problem is linear, hence the least squares (LS) estimator can be applied. In the scenario where only the BS positions are given, the optimization problem becomes nonlinear, thus an iterative nonlinear least squares (NLS) estimator is used.

Due to the short simulation time, both sensor positions and clock offsets are considered to be static. In a real-world application, sensor positions are dynamic, and clock drift is present, requiring sequential estimators or tracking algorithms. This is not regarded in the simulations of this paper.

III. SYNCHRONIZATION IN LONG-TERM EVOLUTION

Long-Term Evolution, marketed as 4G technology, enhances the capabilities of 3G radio access networks (RAN). LTE BSs, or evolved node Bs, support bandwidths of 1.4 to 20 MHz and utilize orthogonal frequency-division multiplexing (OFDM) for the downlink signals [16].

The PSS is a crucial component of the LTE frame structure, used for cell search and initial synchronization of the user equipment (UE). The PSS consists of a Zadoff-Chu (ZC) sequence of length 63, known for its optimal auto-correlation

properties and low cross-correlation with other sequences [17]. These properties make ZC sequences particularly suitable for synchronization purposes. The ZC sequence is generated as

$$s_u^{\text{ZC}}[n] = e^{-i\pi u \frac{n(n+1)}{N_{\text{ZC}}}}, \quad n = 0, 1, \dots, N_{\text{ZC}} - 1, \quad (6)$$

where u is the root index for the sequence, and N_{ZC} the sequence length. In LTE, only the root indices $u \in \{25, 29, 34\}$ are used, allowing for detection by correlation with all predefined sequences. While the sequence length is 63, the 32nd sample is omitted since it is transmitted on the DC carrier frequency [17]. The PSS is transmitted in the central 62 subcarriers of the LTE downlink signal during the last OFDM symbol of the first and sixth subframes in the frequency-division duplex (FDD). This periodic transmission allows UEs to detect the presence of a cell and determine the start of the LTE subframe to achieve symbol time synchronization with the BS. The cell identity within a group is determined by the PSS, making the PSS important for BS identification [18].

IV. SIMULATION SETUP

This section describes the setup of the simulation environment and the performed experiments.

A. Primary Synchronization Signal Generation

In the conducted simulations, LTE BSs with a system bandwidth of 20 MHz and a 30.72 MHz sampling frequency are considered, yielding OFDM symbols containing 2048 samples, excluding the cyclic prefix (CP). A ZC sequence with root index 29 and length 63 is used to generate the PSS. After omitting the 32nd sample, the sequence is symmetrically zero-padded to 2048 samples and the inverse discrete fourier transform is used to OFDM-modulate the time-domain complex baseband signal. This signal is inserted into the specific time slots of the FDD mode.

B. Signal Channeling & Noise Generation

The generated signal is modeled using a free space propagation model and time delayed using a fractional delay filter to allow for subsample delays [19]. In addition, a random phase component is added modeling incoherent oscillators at the transmitter and receiver. No signal attenuation is modeled, instead the noise is amplified to the desired signal-to-noise ratio (SNR). Multipath propagation is not considered in this paper.

C. Signal Detection

The received signal is correlated with a local PSS. Peaks exceeding a predefined threshold are extracted. Additional constraints on peak separation are set since the cyclic time of the signal is known. Quadratic three-point interpolation is used to improve arrival-time measurements to subsample accuracy.

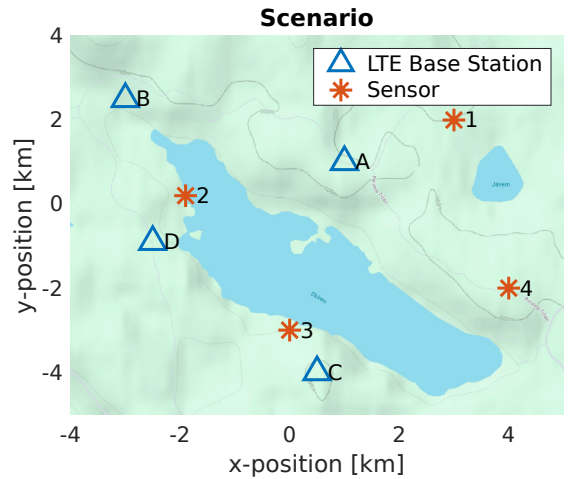


Fig. 1: A visualization of a scenario, where the BSs are marked with blue triangles (Δ) and the sensors are marked with red stars (*). The sensors are part of a cooperating and distributed sensor network.

D. Evaluation

The simulation time was 50 ms, resulting in ten cyclic transmission of the PSS. An example scenario can be seen in Fig. 1. In total, 1000 scenarios of a 10 km by 10 km area were generated according to the following steps:

- 1) The number of BSs was uniformly sampled within the range of four to seven.
- 2) The first four BS positions were uniformly randomized within each quadrant of the simulation area.
- 3) Any additional BSs were uniformly randomized within the whole area.
- 4) BS positions were resampled if the minimum separation was less than a distance of three kilometers.
- 5) Ten sensor positions were uniformly randomized within the whole area. Each sensor was given a uniformly randomized clock offset within a deviation of half a cyclic time of the synchronization signal.

The above listed constraints on BS positions were implemented to mimic the geometries promoting good coverage, which is the case in real LTE networks.

Four experiments were made, in each turn varying the parameters

- a) SNR,
- b) uncertainty in sensor position,
- c) uncertainty in BS position,
- d) disturbances to LTE network synchronization.

V. HARDWARE EXPERIMENTS

Hardware experiments were performed using two software defined radios, specifically the USRP B205mini-i from Ettus Research, see Fig. 2, corresponding to a BS with a 1.4 MHz bandwidth and a sensor. The transmission port of the BS was connected via an SMA cable to the receiver port of the sensor. The maximal transmission power of the USRP is 20 dBm (0.1 W), but fixed attenuators corresponding to 58 dB were

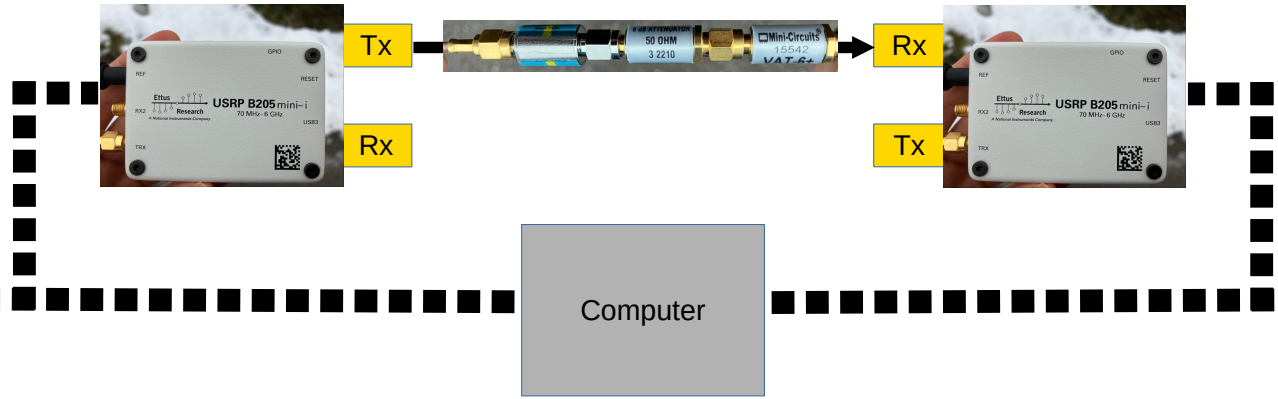


Fig. 2: Block diagram for the setup of the hardware experiments. Two USRPs were connected using SMA cable via a set of attenuators corresponding to 58 dB of attenuation. The left USRP corresponds to the LTE BS and the right USRP to a sensor within the sensor network. The computer is used for generating the LTE signals and saving data.

used to dampen the signal in the channel. Both USRP devices were connected via USB to a computer. A block diagram of the setup can be seen in Fig. 2. The open source project srsRAN [20] was utilized to generate the LTE downlink signals and save timestamped transmitted and received I/Q data, using a sample rate of 1.92 MHz at both ends. A recording of 1.75 seconds was captured, corresponding to around 350 PSS detections. In the post-processing, an LS estimator was used for estimating the time synchronization of the sensor using the SWINS method.

VI. RESULTS & DISCUSSION

In this section, the simulation experiments are presented followed by the result for the hardware experiment.

A. Signal-to-Noise Ratio

Experiments were performed using the reception times acquired using different noise levels to investigate noise and jamming effects on time synchronization performance. The initial results indicated initialization issues for both methods, especially for the nonlinear estimator. The error distribution, see Fig. 3, for the NLS at 20 dB SNR shows a large set of outliers, especially for RBS. This is most probably a result of the convergence to local minimas for the optimization algorithm. In addition, the main lobe for the error distribution is wider which indicates a larger measurement variance for RBS. The variance is a result of the noise affecting the cross-correlation and thereby the arrival time measurements. Since large outlier errors significantly affected the clock offset error, an outlier rejection threshold of 400 nanoseconds (ns) was chosen yielding the results in Fig. 4. The introduced threshold removes 0.04% – 0.08% of the data points.

Both methods show decreased performance with a decrease in SNR. SWINS outperforms RBS, due to the lower measurement variance. RBS combines the uncertainty of the signal arrival times yielding an increase in measurement variance. In addition, RBS suffers from initialization issues to a larger

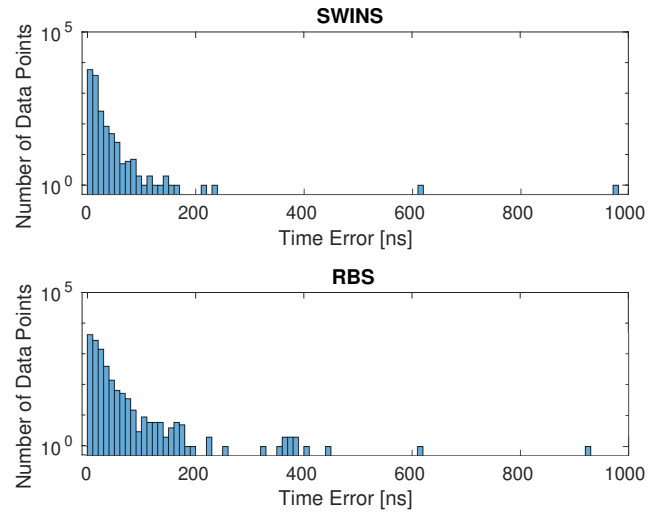


Fig. 3: Histogram of the time synchronization error using the NLS, jointly estimating the sensor clock offset and position at 20 dB SNR. In the uppermost plot, the error distribution for SWINS is shown. In the downmost plot, the error for RBS is illustrated. Note that the logarithmic scaling of the y-axis. The bin width is 10 ns. Also note that errors with larger magnitudes than 1000 ns exist.

extent. The performance of SWINS is better than GPS, except for the case with estimated sensor positions, using NLS, at low SNR. For sole clock offset estimation, i.e., with known sensor positions, RBS performs better than GPS. However, joint estimation of clock offset and sensor position using the NLS performs worse than GPS. Note that the performance of GPS is using the publicly available signals, not utilizing the restricted P -code. Noteworthy, the GPS performance is probably SNR dependent, but no such information was found.

B. Sensor Position Uncertainty

Experiment were performed using varying sensor position uncertainty to find the pivot point for using joint estimation of the clock offset and sensor position instead of sole clock

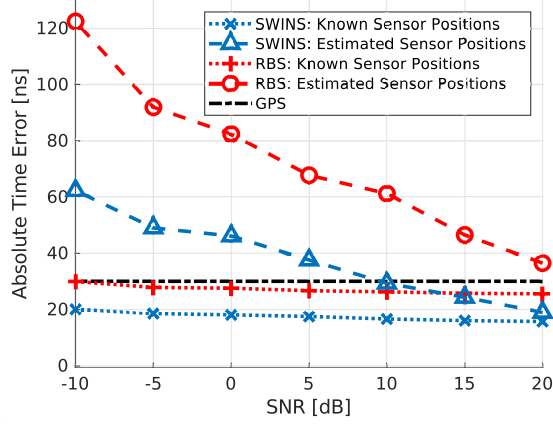


Fig. 4: Comparison of GPS and the 95th percentile estimator performance as a function of SNR. Note that the 95% GPS performance is likely SNR dependent, although this is not visualized in the graph. Errors larger than 400 ns were considered as outliers and hence excluded. The outliers correspond to 0.04% – 0.08% of all data points depending on the method and SNR.

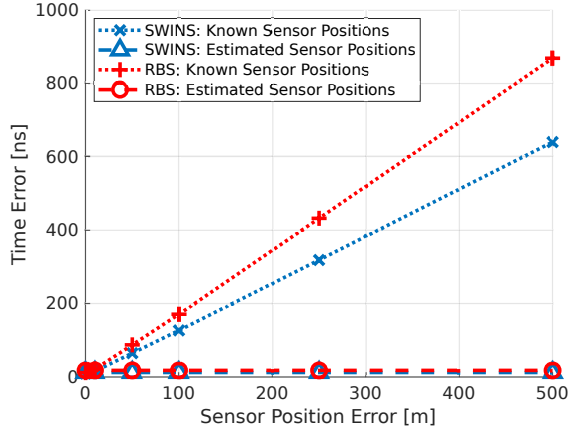


Fig. 5: Average time synchronization error as a function of uncertainty in sensor position at 20 dB SNR. The estimator with estimated sensor position is unaffected by the injected disturbance.

offset estimation. A plot of the sensitivity can be seen in Fig. 5. The LS estimators for both methods were affected linearly. Simulations indicate that SWINS is more robust to sensor position uncertainties than RBS for sole clock offset estimation. Joint estimation of clock offset and sensor position is superior to sole clock offset estimation when the sensor position uncertainty exceeds 5 and 7 meters for SWINS and RBS respectively. The estimator pivot points and the gradients at the pivot points are presented in Tab. I.

C. LTE Base Station Position Uncertainty

In addition to sensor position uncertainty, the impact of BS position uncertainty was analyzed. The sensitivity for each method is illustrated in Fig. 6. The simulations exhibit similar sensitivity for the LS estimators. However, for RBS, the NLS estimators are more sensitive compared to the corresponding results for SWINS. The larger the uncertainty grows, the larger the gradient becomes. Depending on the application

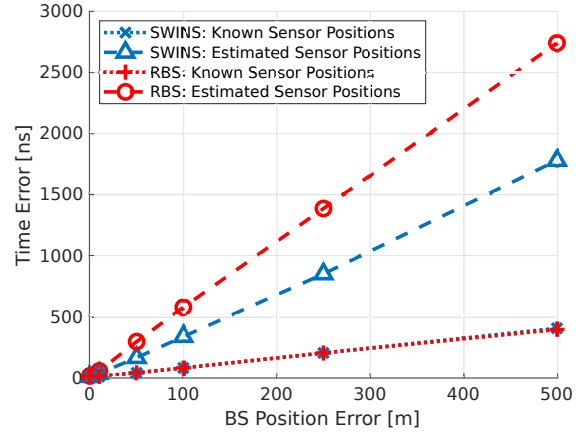


Fig. 6: Average time synchronization error as a function of uncertainty in BS position at 20 dB SNR. The estimator utilizing sensor position is less affected.

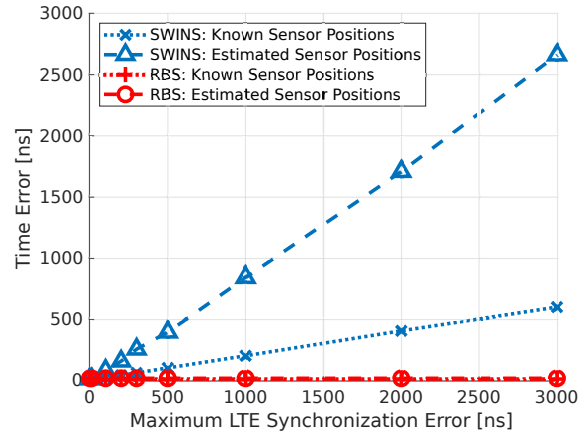


Fig. 7: The average time synchronization error as a function of the synchronization disturbance in the LTE network at 20 dB SNR. Both SWINS estimators are affected, while RBS is completely unaffected.

Tab. I: The table shows the uncertainty pivot point and the pivot point error gradient for the LS to the NLS estimator, based on the sensor position uncertainty at 20 dB SNR.

	Pivot point [m]	Err. grad. [$\frac{ns}{m}$]
SWINS	5	0.65
RBS	7	0.94

and the time synchronization performance requirements, a certain maximum BS uncertainty is required to satisfy the prerequisites.

D. LTE Network Synchronization

Since GNSS-denial could cause disturbances to the LTE network synchronization, experiments were performed using varying clock synchronization offsets of the BSs while assuming synchronous transmissions. The results in Fig. 7 showcase a linear dependence between the synchronization error in the LTE network and the clock offset estimation for SWINS,

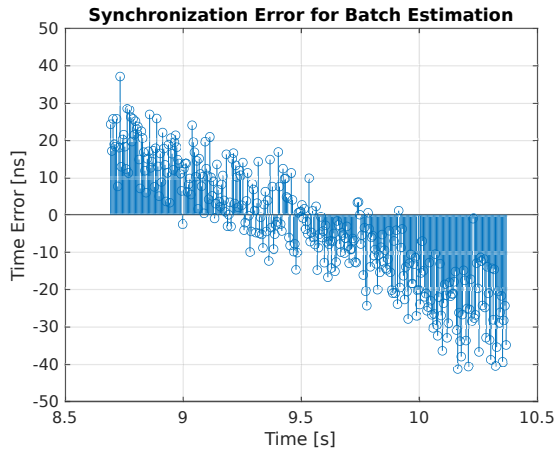


Fig. 8: Time synchronization error for the hardware experiments using a batch estimator with the whole recorded data set. The estimation drifts with time.

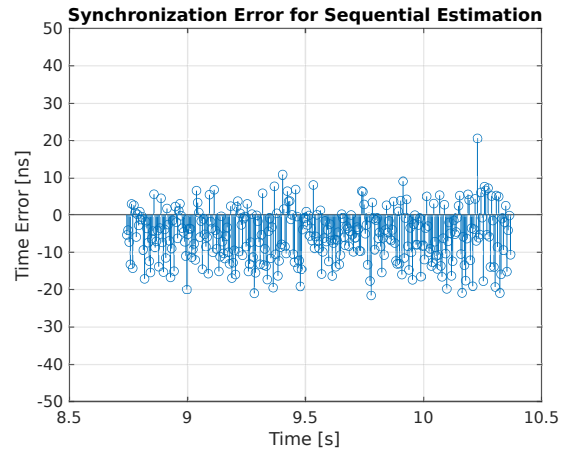


Fig. 9: Time synchronization error for the hardware experiments using a sequential estimator with a batch size of ten. The estimate does not drift with time.

while RBS is unaffected by the disturbances. This is a major advantage, which can be exploited to maintain performance for non-synchronous reference signals. However, there are other protocols, e.g., IEEE 1588 Precision Time Protocol (PTP) and Synchronous Ethernet (SyncE), allowing the LTE network to remain synchronized in situations with GNSS-denial [21].

Assuming that the LTE network is non-synchronous, drift within the LTE network is probably present. Equivalently, measurements supporting the evidence of drift in the arrival of the PSS from different BSs implies evidence for a non-synchronous LTE network. Further investigation of methods for measuring the synchronization of the LTE network is needed.

E. Hardware

To verify the simulation results, hardware experiments were carried out to ensure method performance when using the full LTE protocol stack. Note that only one BS and one sensor were used.

Fig. 8 shows the clock offset error when using the whole recording for estimation. Observing the graph, it becomes clear that the disparity in local oscillator frequency causes drift in the time synchronization estimation error. Thus, a large batch size is not preferred. Using a sequential LS estimation algorithm, the drift in the estimation error can be mitigated, see Fig. 9. Estimation using a batch size of ten results in an average absolute error of 7.4 ns. Another way of dealing with the oscillator drift is using tracking algorithms. Besides drift, the estimate seems a bit biased towards negative errors, see Fig. 9. One potential source of bias is the timestamp insertion which occurs 100 samples prior to transmission to account for the delay in the antenna. If not calibrated, this could cause a bias in the error calculations.

VII. CONCLUSIONS

This study has demonstrated that LTE-based time synchronization methods can achieve accuracy comparable to when

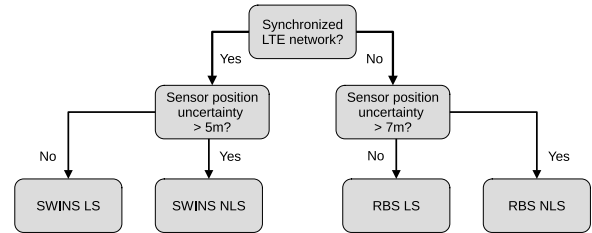


Fig. 10: Flow chart, based on the simulation results, for choosing the preferred method and estimator depending on the circumstances.

using the publicly available GNSS signals. Hence, demonstrating that the method could solve the time synchronization in a GNSS-denied environment. The passive SWINS method is preferable in synchronized LTE networks due to its increased accuracy, lower measurement covariance, and stealth properties, while the active RBS method is superior to SWINS in unsynchronized LTE networks. In addition, joint estimation of clock offset and receiver position is preferred if the receiver position uncertainty exceeds 5 and 7 meters for SWINS and RBS respectively. A guideline for choosing method and estimator can be seen in Fig. 10. The BS position uncertainty effect on time synchronization performance follows a linear relationship with approximately 0.7–5.5 ns per meter of uncertainty, depending on method and estimator, which highlights the importance of BS location accuracy.

The hardware experiments showcased good method performance in a simplified scenario setup. Furthermore, we have demonstrated that it is necessary to deal with oscillator drift to avoid degrading performance.

Further research and real-world testing for more complex scenarios are recommended to validate these findings. Enhancements to the investigated methods can be done by incorporating the CRS in the LTE downlink. In addition, methods for determining the synchronization of LTE networks are of interest to adaptively switch synchronization method, based on the LTE network conditions.

REFERENCES

- [1] G. Andersson, P. Donalek, R. Farmer, N. Hatzigiorgiou, I. Kamwa, P. Kundur, N. Martins, J. Paserba, P. Pourbeik, J. Sanchez-Gasca, R. Schulz, A. Stankovic, C. Taylor, and V. Vittal, "Causes of the 2003 major grid blackouts in North America and Europe, and recommended means to improve system dynamic performance," *IEEE Transactions on Power Systems*, vol. 20, no. 4, pp. 1922–1928, 2005.
- [2] J. Amelot, D. Anand, T. Nelson, G. Stenbakken, Y.-S. Li-Baboud, and J. Moyne, "Towards Timely Intelligence in the Power Grid," in *Proceedings of the 44th Annual Precise Time and Time Interval Systems and Applications Meeting*, pp. 399–412.
- [3] D. Egea, M. Arizabaleta, T. Pany, F. Antreich, J. A. López-Salcedo, M. Paonni, and G. Seco-Granados, "GNSS User Technology: State-of-the-Art and Future Trends," *IEEE Access*, vol. 10, pp. 1–1, 01 2022.
- [4] X. Yang, F. Chen, W. Liu, and F. Wang, "Analysis of the Effect Jammer Types on GNSS Receiver Measurements," in *2019 IEEE 2nd International Conference on Information Communication and Signal Processing (ICICSP)*, 2019, pp. 117–120.
- [5] A. Hult, "Time Synchronization of TDOA Sensors Using a Local Reference Signal," Master's thesis, Division of Communication Systems Department of Electrical Engineering, Linköping University, Linköping, Sweden, 2020.
- [6] E. Grigoriou, "A Survey of Quality of Service in Long Term Evolution (LTE) Networks," in *Enabling Technologies and Architectures for Next-Generation Networking Capabilities*, M. Elkhodr, Ed. IGI Global, 2019, pp. 125–146.
- [7] X. Yang, Y. Xiong, G. Jia, W. Fang, and X. Zheng, "PSS based time synchronization for 3GPP LTE downlink receivers," in *2011 IEEE 13th International Conference on Communication Technology*, 2011, pp. 930–933.
- [8] S. Cai, Z. Duan, and J. Jiang, "Methods of Time Offset Estimation and Performance Evaluation of Synchronization for 3GPP LTE Downlink," in *2009 Pacific-Asia Conference on Circuits, Communications and Systems*, 2009, pp. 135–138.
- [9] M. Driusso, C. Marshall, M. Sabathy, F. Knutti, and H. Mathis, "Vehicular Position Tracking Using LTE Signals," *IEEE Transactions on Vehicular Technology*, vol. 66, no. 4, 2017.
- [10] M. Arizabaleta-Diez, M. S. Hameed, and T. Pany, "LTE transmitter location and clock state estimation: Simulated and real measurements using the SSS and CRS signals," in *Proceedings of the 35th International Technical Meeting of the Satellite Division of The Institute of Navigation (ION GNSS+ 2022)*, 2022, pp. 2444–2463.
- [11] Z. Z. M. Kassas, J. Khalife, K. Shamaei, and J. Morales, "I hear, therefore i know where i am: Compensating for gnss limitations with cellular signals," *IEEE Signal Processing Magazine*, vol. 34, no. 5, pp. 111–124, 2017.
- [12] Y. Wang, H. Zhu, T. Liang, and J. Qian, "Signals of Opportunity Navigation Using LTE Downlink Signals," in *2022 IEEE 22nd International Conference on Communication Technology (ICCT)*, 2022, pp. 1070–1074.
- [13] D. Zachariah, S. Dwivedi, P. Händel, and P. Stoica, "Scalable and Passive Wireless Network Clock Synchronization in LOS Environments," *IEEE Transactions on Wireless Communications*, vol. 16, no. 6, pp. 3536–3546, 2017.
- [14] J. Elson, L. Girod, and D. Estrin, "Fine-grained network time synchronization using reference broadcasts," *SIGOPS Oper. Syst. Rev.*, vol. 36, no. SI, p. 147–163, dec 2003. [Online]. Available: <https://doi-org.e.bibl.liu.se/10.1145/844128.844143>
- [15] M. Roche, "Time Synchronization in Wireless Networks," https://www.cse.wustl.edu/~jain/cse574-06/ftp/time_sync/index.html, accessed: 2024-04-18.
- [16] B. Asp, K. Fors, J. Nilsson, and K. Wiklundh, "Särbarhetsaspekter vid militär användning av LTE," Totalförsvarets Forskningsinstitut, Tech. Rep., 2016.
- [17] J. G. Andrews, "A Primer on Zadoff Chu Sequences," 5 Jun 2023, preprint at webpage: <https://arxiv.org/pdf/2211.05702.pdf>.
- [18] L. Nasraoui, "Advanced Synchronization Techniques for OFDM Systems," Ph.D. dissertation, Université de Carthage, 2015.
- [19] V. Valimaki and T. Laakso, "Principles of fractional delay filters," in *2000 IEEE International Conference on Acoustics, Speech, and Signal Processing. Proceedings (Cat. No.00CH37100)*, vol. 6, 2000, pp. 3870–3873 vol.6.
- [20] SRSRAN, "Open Source 4G/5G from Software Radio Systems (SRS)," accessed: 2025-01-07. [Online]. Available: <https://github.com/srsran>
- [21] A. Telecom, "Synchronization & Mobile networks," Tech. Rep., 2016. [Online]. Available: <https://www.albedotelecom.com/src/lib/WP-Mobile-PTP.pdf>